

Long plasma channels generated by femtosecond laser pulses

H. Yang,¹ J. Zhang,^{1,*} W. Yu,² Y. J. Li,¹ and Z. Y. Wei¹

¹Laboratory of Optical Physics, Institute of Physics, Chinese Academy of Sciences, Beijing 100080, China

²Shanghai Institute of Optics and Fine Mechanics, Chinese Academy of Sciences, Shanghai 230026, China

(Received 16 November 2000; revised manuscript received 4 June 2001; published 17 December 2001)

Generation of a long plasma channel by femtosecond laser pulses is investigated. The results show that the balance between the nonlinear self-focusing of the laser beam and plasma defocusing forms a long plasma channel, which guides the laser beam to propagate a long distance in air. This phenomenon can be used to trigger lightning.

DOI: 10.1103/PhysRevE.65.016406

PACS number(s): 52.38.-r

I. INTRODUCTION

Propagation of intense short laser pulses over a long distance in gases and plasmas has been studied at different laboratories [1–4]. The propagation of intense laser pulses is important in a wide range of applications, such as guiding a very long electrical discharge for triggering lightning. Natural lightning is very harmful to humankind, and causes huge financial losses. For example, the power industry loses a few billion dollars every year because of lightning strikes. One possible way of protecting dedicated facilities from lightning strikes is to divert the lightning to a safe place.

The control of lightning was envisioned by Benjamin Franklin when he conducted his legendary experiments in 1752. A modern method for triggering lightning is to fire small rockets trailing ground wires toward thunder clouds. However, its success rate is only about 60%. Moreover, it cannot be launched on a semicontinuous basis. Laser-triggered lightning was proposed by Ball in 1974 [5], but it was not successful due to the limitation of the laser technology at that time. Japanese researchers in Osaka reported experiments of successful triggered lightning using 2-kJ CO₂ laser pulses [6]. As a result of the progress in chirped pulse amplification (CPA) technology, we can now obtain intense ultrashort laser pulses from table-top laser systems. The laser intensity can reach the order of 10^{19} W cm⁻². This provides a promising way to generate a long plasma channel to trigger lightning.

The formation of the long plasma channels is attributed to the balance of self-focusing and defocusing of the laser beam, due to the intensity-dependent nonlinear index of air and the axial plasma filaments created by tunneling ionization of air, respectively. Braun *et al.* [7] observed that ultrashort laser pulses can be self-channeled into a filament with an intensity of 7×10^{13} W cm⁻² and propagate through a distance greater than 20 m. The average electron density in the channel was found to be around 10^{17} cm⁻³. The long filaments provide a channel with enhanced conductivity that could initiate and guide lightning. In this paper, we use a one-dimensional (1D) propagation code to simulate this pro-

cess and obtain results in agreement with experimental measurements.

II. PRINCIPLE OF FORMING A LONG PLASMA CHANNEL

The formation of a long plasma channel in air is of key importance for laser-triggered lightning. In vacuum, the propagation distance of a Gaussian laser beam is confined to the Rayleigh length $Z_R = kr_0^2/2$, where r_0 is the laser spot size at focus and k is the wave number. Generally, high laser intensities require tight focusing, which in turn results in very short propagation distance (e.g., when $r_0 = 80$ μm and $\lambda = 0.8$ μm, the Rayleigh length is only $Z_R = 25$ mm). However, we shall show that it is possible for a laser beam to propagate over a greatly extended distance (many Rayleigh lengths) in air. We find that the laser propagation in the air is strongly affected by the nonlinear self-focusing and ionization-induced defocusing effects. The balance between these two effects can guide the propagation of laser pulses and create a long plasma channel.

The wave equation for laser propagation in a medium can be written as [8–10]

$$\nabla^2 E - \frac{1}{c^2} \frac{\partial^2}{\partial t^2} E = k^2 (1 - \eta^2) E, \quad (1)$$

with the refractive index

$$\eta = 1 + \eta_2 I - n_e / 2n_c. \quad (2)$$

For air at 1 atm we have $\eta_0 = 1$ and the nonlinear index $\eta_2 = 5 \times 10^{-19}$ cm² W⁻¹, $I = (c/8\pi)|E|^2$ is the laser intensity, n_e is the density of free electrons, and $n_c = m_e \omega^2 / 4\pi e^2$ is the plasma critical density. The second term in Eq. (2) describes the optic-field-induced nonlinear self-focusing in gas, which can be attributed to the fact that the central part of the beam, having higher intensities, experiences a larger refractive index than the beam edge. The third term describes ionization-induced defocusing, since there are more free electrons in the central part of the beam.

Let us consider a Gaussian laser beam focused upon the opening of a gas chamber with a field strength E_0 and a minimum spot size r_0 . Assuming the wave amplitude varies slowly compared to the laser wavelength, the laser beam remains approximately Gaussian during its propagation in the gas. It can be expressed as

*Author to whom correspondence should be addressed. Email address: jzhang@aphy.iphy.ac.cn

$$|E(r,y)| = E_0(r_0/r_s) \exp(-r^2/2r_s^2), \quad (3)$$

where we neglect the energy loss during propagation in Eq. (3), $r_s(z)$ is the spot size at which the field strength reduces to e^{-1} of its peak value at the propagation axis, and r_0 is the laser beam waist at $z=0$. The variation of the spot size in the propagation direction is given by

$$d^2r_s/dz^2 = (\partial\eta/\partial r)_{r_s} + 4/k^2r_s^3, \quad (4)$$

where η is a function of $|E|$ and

$$\partial\eta/\partial r = (\partial\eta/\partial|E|)(\partial|E|/\partial r) = -(2r/r_s^2)(|E|\partial\eta/\partial|E|).$$

We have assumed that around the spot size the factor of $(|E|\partial\eta/\partial|E|)$ is slowly varying with r .

When laser intensity is $I \geq 10^{14} \text{ W cm}^{-2}$, tunnel ionization dominates the ionization process [11–17]. According to the tunneling model, the ionization rate is given by

$$dn_e(t)/dt = w(t)(N_0 - n_e), \quad (5)$$

where $n_e(t)$ is the time-dependent electron density, N_0 is the initial neutral gas density, and $w(t)$ is given by

$$w(|E|) = 4\Omega \left(\frac{E_i}{E_h} \right)^{5/2} \frac{E_a}{|E|} \exp \left[-\frac{2}{3} \left(\frac{E_i}{E_h} \right)^{3/2} \frac{E_a}{|E|} \right], \quad (6)$$

where E_i and E_h are the ionization potential of the gas under consideration and of hydrogen, respectively, $\Omega = me^2/h^3 = 4.16 \times 10^{16} \text{ s}^{-1}$ is the atomic frequency, and $E_a = m^2e^5/h^4 = 5.1 \times 10^9 \text{ V cm}^{-1}$ is the field strength at the Bohr radius. For simplicity, considering a flat-top laser pulse beam in the time domain, the density of ionized electrons can be expressed as

$$n_e = N_0 [1 - \exp(-w(|E|\tau))], \quad (7)$$

where τ is the duration of laser pulses. From the above equations we get

$$\frac{d^2R}{d^2Z} = \left(1 - \alpha \frac{P}{P_N} \right) R^{-3} + \frac{(DR-1)}{\exp(DR + FDR/\exp(DR))}, \quad (8)$$

where $\alpha = 4/e$, $R = r_s/r_0$, $Z = z/z_R$, $A = E_i/E_h$, $B = E_a/E_0$, $C = N_0\Omega\tau k^2 r_0^2 A^{5/2} B e^{1/2}/n_c$, $D = 2A^{3/2}B \exp(0.5)/3$, $F = 6\Omega A\tau$, P is the laser power, and $P_N = 2\pi/k^2\eta_2$ is the critical power for nonlinear self-focusing.

We have now obtained the equation describing the variation of spot size R with respect to propagation distance Z . The first term on the right-hand side of the equation is responsible for the nonlinear self-focusing and the second term for the plasma defocusing. A proper balance between the two effects could be used to guide the laser propagation over a long distance.

III. CALCULATION RESULTS

We have assumed that the incident laser beam is focused upon the opening of a gas chamber. If there is no gas inside

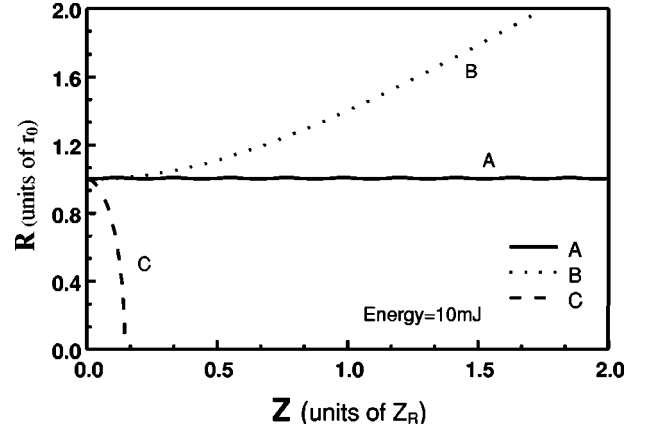


FIG. 1. Variation of the laser-beam radius with the propagation distance Z . The dashed curve (C) is self-focusing without ionization; the solid curve (A) represents propagation of a laser pulse in air; the dotted curve (B) is free propagation in vacuum ($r_0 = 180 \mu\text{m}$, $\tau = 150 \text{ fs}$).

the chamber, the laser beam will diffract with its spot size increasing monotonically with Z , as shown in Fig. 1 by the dotted curve (B). If there is gas inside but without any ionization processes, the propagation of the laser beam in the atomic gas is governed by

$$d^2R/dZ^2 = (1 - \alpha P/P_N)R^{-3}. \quad (9)$$

Its solution can be written as

$$R^2 = 1 + (1 - \alpha P/P_N)Z^2, \quad (10)$$

where we have assumed that $R = 1$ and $Z = 0$. When the laser power is $P > P_N/\alpha$, the laser beam will be self-focused with a spot size decreasing monotonically during propagation, as shown by the dashed curve (C) in Fig. 1. According to Eq. (10), when $Z = (\alpha P/P_N - 1)Z_R$, the spot size R reduces to zero and a singularity in field strength occurs. In reality, this will not happen since the enhancement in field strength will inevitably lead to ionization. The solid curve (A) in Fig. 1, calculated from Eq. (8) with $r_0 = 180$ (we can get this with a lens), pulse energy $E = 10 \text{ mJ}$ ($P = 67 \text{ GW}$), $\tau = 150 \text{ fs}$, and a laser wavelength of 800 nm , shows the real situation for the propagation of an intense laser beam in ionizing gases. The variation of the beam radius R with the propagation distance Z is presented. It shows that the beam radius remains almost constant (about $180 \mu\text{m}$), and the slight oscillation reflects the competition between self-focusing and defocusing. When the laser beam is focused to a certain extent, the tunneling ionization rate increases. The ionized electrons make the beam defocused. Because of defocusing, the ionization rate will decrease. The nonlinear effect in gases will then make the beam focused again. We find the laser intensity inside the channel to be about $10^{14} \text{ W cm}^{-2}$ in Fig. 2 (curve A), close to the threshold of the tunnel ionization of air. This result agrees with the measurements in Ref. [7], in which the laser intensity in the channel was measured to be $7 \times 10^{13} \text{ W cm}^{-2}$. Curves B and C in Fig. 2 correspond to the laser intensity of Fig. 1 (curves B and C). From Eq. (8), we

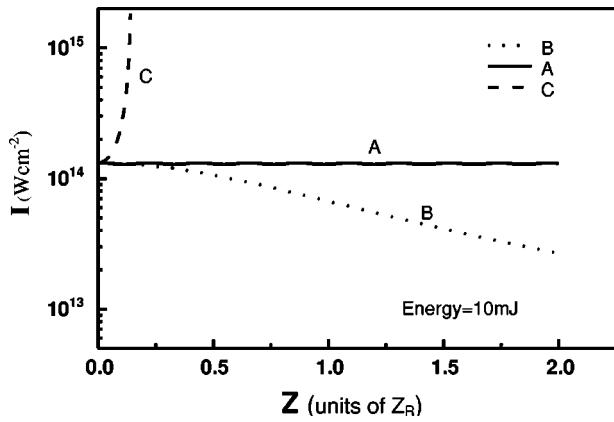


FIG. 2. The laser intensity in the channel versus the propagation distance ($r_0 = 180 \mu\text{m}$, $\tau = 150 \text{fs}$).

simulate variation of the laser beam radius with the input laser pulse energy (power). The results are shown in Fig. 3. The behavior of the laser propagation is sensitive to the input laser energy (power). Only the laser energy (power) in the range shown by curves *B*, *C*, *D*, and *E* in Fig. 3 can lead to an oscillated propagation of the laser beam to a very large distance (many Rayleigh lengths). A channel length larger than 20 m was observed in the experiment in Ref. [7]. In order to show the characteristics of the channel more clearly, we only draw a short range covering two Rayleigh lengths in Figs. 1–3. Characters of the plasma channels formed are different because of a variation of the laser power. From curves *B*, *C*, *D*, and *E* in Fig. 3, there must exist an energy (power) which can cause the laser-beam radius to keep a constant (such as curve *C*). The oscillation amplitude of the laser-beam radius becomes very large when the laser power departs from this power. So the small disturbance would cause the laser beam to spread and the laser beam could not propagate a very long distance. Furthermore, this would generate a discontinued distribution of electrons in the channel (as shown in Fig. 5 and Fig. 6). For a too high or too low laser power, the laser beam would spread as curves *A* and *F* in Fig. 3.

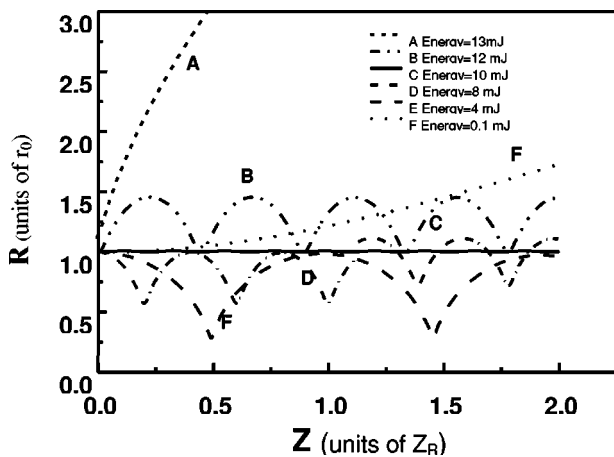
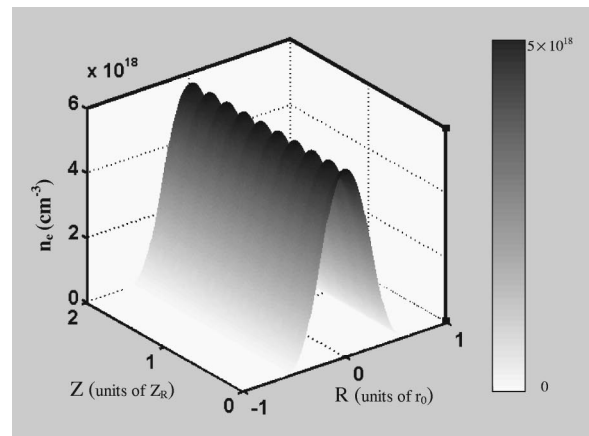
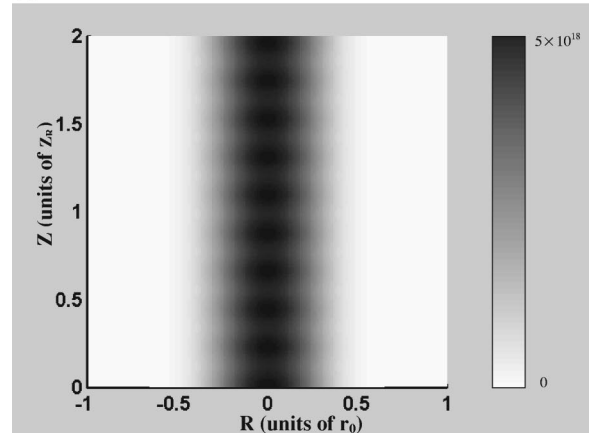


FIG. 3. The laser-beam propagation for different initial energy ($r_0 = 180 \mu\text{m}$, $\tau = 150 \text{fs}$).



(a)



(b)

FIG. 4. Spatial distribution of the electron density in the plasma channel. (a) represents the distribution of the electrons in the channel. (b) is the contour curve of the electron density (the pulse energy $E = 10 \text{mJ}$, $r_0 = 180 \mu\text{m}$, and $\tau = 150 \text{fs}$).

The density of ionized electrons in the channel also oscillates along Z as shown in Fig. 4(a) and Fig. 4(b) corresponding to Fig. 1 (curve *A*). The electron density is semicontinuous and the maximum density at the center of the plasma

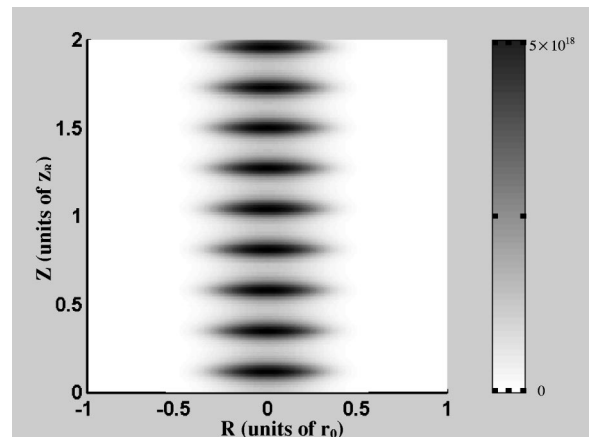


FIG. 5. The contour curve of the electron density in the plasma channel with the pulse energy $E = 12 \text{mJ}$ ($r_0 = 180 \mu\text{m}$, and $\tau = 150 \text{fs}$).

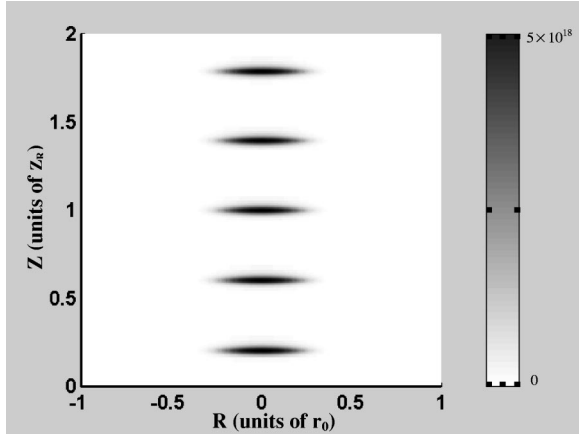


FIG. 6. The contour curve of the electron density in the plasma channel with the pulse energy $E=4$ mJ ($r_0=180$ μm , and $\tau=150$ fs).

channel can reach 10^{18} cm^{-3} , while the average electron density is about 10^{17} cm^{-3} . An average electron density of about 6×10^{16} cm^{-3} was measured by Braun *et al.* [7] in the laser channel. We find that the radius of the ionized channel in Fig. 4 is about 40–50 μm and is a quarter radius of the initial laser beam. In the calculation, we find that the plasma channel can be discontinued like beads when the laser power largely departs from the optimum energy (power). For example, if the laser pulse energy $E=12$ mJ or $E=4$ mJ, the plasma channel would be discontinued as shown in Fig. 5 and Fig. 6.

In the above calculations, we did not consider the loss of the laser energy in the propagation, because usually this energy loss is very small. In the propagation process, the main energy loss is due to the ionization. Assuming the plasma channel is in a column configuration and taking the average laser intensity to be $I=10^{14}$ W/cm^2 , the energy loss is

$$E_{\text{loss}} = 1.6 \times 10^{-19} \bar{n}_e \pi d_0^2 L U_i / 4. \quad (11)$$

If we take the ionized channel $L=1$ m, $d=80$ μm (the ionized channel diameter is about a quarter of the laser beam diameter from Fig. 4), and assume $\bar{n}_e=6 \times 10^{16}/\text{cm}^3$ (in Ref. [7]), the ionization energy is $U_i=15.5$ eV, and the energy loss is

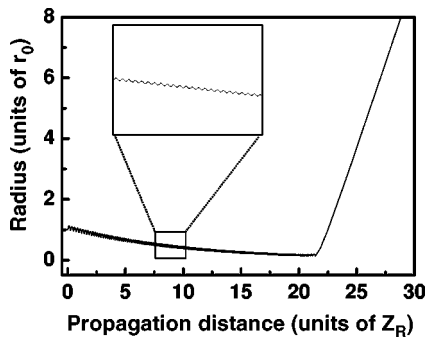


FIG. 7. The propagation of a laser beam taking into account the loss of the laser energy. The inset shows details of a portion of the magnified plasma channel.

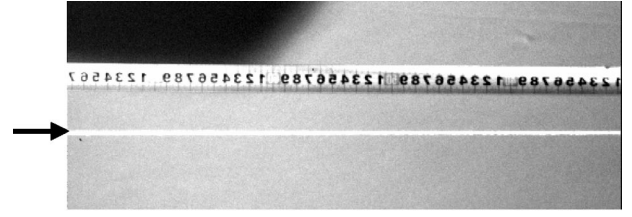


FIG. 8. One portion of the laser plasma channel taken by a CCD camera.

$$E_{\text{loss}} = 0.74 \text{ mJ}.$$

We find that the energy loss is relatively small compared with the total input energy. The electron density in the channel is almost uniform with our stimulation in Fig. 4. We believe the laser energy decays approximately linearly and the laser energy with propagation distance becomes

$$\varepsilon(z) = \varepsilon(0)(1 - \beta z), \quad (12)$$

where β is the laser energy decay coefficient per Rayleigh length and $\varepsilon(0)$ is the initial laser energy. Following the above evaluation of the energy depletion and Eq. (12), we can get $\beta=0.094$ per Rayleigh length. Because β is very small, the $\varepsilon(z)$ can be written as

$$\varepsilon(z) \approx \varepsilon(0) \exp(-\beta z).$$

Therefore, the amplitude of Eq. (3) has to be multiplied by $\exp(-\beta z/2)$. We can get new simulation results of laser propagation from Eq. (8) shown in Fig. 7. From it we find that the radius of the channel begins to decrease and finally collapse. This appearance is caused by a decay of the energy. The laser beam has to keep the balance of the focusing and defocusing by decreasing the radius. At last, this balance becomes unstable when the depletion of laser energy becomes large enough. Smaller laser radius and depletion of energy would lead to the collapse of the laser beam. In the stimulation process, we let $\beta=0.094$, $\tau=150$ fs, and $\varepsilon(0)=10$ mJ. From Fig. 7, we know that the laser beam can propagate longer than 20 Rayleigh lengths and collapse (for a laser beam of $r_0=180$ μm , the corresponding Rayleigh length is $Z_R=12.7$ cm). In order to show this more clearly, we magnify a small part of the channel as the inset in Fig. 7. The inset gives details for about five Rayleigh lengths in the process of the beam propagation. From it we can observe the oscillation of the beam, as in Fig. 1. Furthermore, in our experimental measurements, we observed a plasma channel longer than 5 m as shown in Fig. 8 (laser parameter $E=15$ mJ, $\tau=25$ fs). Because of the limited imaging range of the CCD camera, only a part of the laser channel can be taken in Fig. 8 (about 50 cm). Moreover, the resistivity of the channel was measured to be smaller than 0.5 Ω cm. Such a long and conductive channel provides a good testbed for the investigation of triggered lightning.

IV. CONCLUSION

A short-pulse laser beam with a Gaussian profile can propagate over a long distance in air due to the balance be-

tween focusing and defocusing of the laser beam. The variation of the beam radius with propagation distance is studied. There exists an optimum energy (power) which can lead the laser beam to propagate a very long distance. It is found that the profile of the electron density in the channel is oscillating and the peak electron density is about 10^{18} cm^{-3} in the channel.

ACKNOWLEDGMENTS

We acknowledge helpful discussions with L. M. Chen, Q. L. Dong, and T. Z. Lu. This work was supported by the National Natural Science Foundation of China (Grant Nos. 19825110 and 10004015) and NKBRFSF (Grant No. G1999075200).

-
- [1] B. La Fontaine, F. Vidal, Z. Jiang, C.Y. Chien, D. Comtois, A. Desparois, T.W. Johnston, J.-C. Kieffer, and H. Pepin, *Phys. Plasmas* **6**, 1615 (1999).
- [2] X.M. Zhao, J.-C. Diels, C.Y. Wang, and J.M. Elizondo, *IEEE J. Quantum Electron.* **31**, 599 (1995).
- [3] S. Tzortzakis *et al.*, *Phys. Rev. E* **60**, R3505 (1999).
- [4] B.M. Penetrante and J.N. Bardsley, *Phys. Rev. A* **43**, 3100 (1991).
- [5] L.M. Ball, *Appl. Opt.* **13**, 2292 (1974).
- [6] T. Yamanaka, Asian Science Seminar on High-power Laser Matter Interaction, Osaka, Japan, 1999.
- [7] A. Braun, G. Korn, X. Liu, D. Du, J. Squier, and G. Mourou, *Opt. Lett.* **20**, 73 (1995).
- [8] Y.R. Shen, *The Principles of Nonlinear Optics* (Academic, New York, 1993).
- [9] R. Fedosejevs, X.F. Wang, and G.D. Tsakiris, *Phys. Rev. E* **56**, 4615 (1997).
- [10] E. Esarey *et al.*, *IEEE J. Quantum Electron.* **33**, 1879 (1997).
- [11] S. Augst, D. Dmeyerhofer, D. Strickland, and S.L. Chin, *J. Opt. Soc. Am. B* **8**, 858 (1991).
- [12] M. Mlejnek, E.M. Wright, and J.V. Moloney, *Phys. Rev. E* **58**, 4903 (1998).
- [13] B. La Fontaine *et al.*, *IEEE Trans. Plasma Sci.* **27**, 688 (1999).
- [14] W.P. Leemans, C.E. Clayton, W.B. Mori, K.A. Marsh, P.K. Kaw, A. Dyson, C. Joshi, and J.M. Wallace, *Phys. Rev. A* **46**, 1091 (1992).
- [15] P. Sprangle, E. Esarey, and A. Ting, *Phys. Rev. A* **41**, 4463 (1990).
- [16] R. Bharuthram, J. Parashar, and V.K. Tripathi, *Phys. Plasmas* **6**, 1611 (1999).
- [17] B. Corkum, N.H. Burnett, and F. Brunel, *Phys. Rev. Lett.* **62**, 1259 (1989).